Detection Sensitivities of Photoluminescence Spectroscopy and Polariscopy to Residual Strains in a (110)-oriented ZnTe Single Crystal: Explore of Strain-sensitivity Inspection Techniques

Hideo Takeuchi

Citation	Physics Procedia. 76; 4-10
Issue Date	2015
Type	Journal Article
Textversion	Publisher
Right	© 2015 The Authors. Published by Elsevier B.V. This is an open access article under the CC BY-NC-ND license (https://creativecommons.org/licenses/by-nc-nd/4.0/)
DOI	10.1016/j.phpro.2015.10.002

TAKEUCHI, H. (2015). Detection Sensitivities of Photoluminescence Spectroscopy and Polariscopy to Residual Strains in a (110)-oriented ZnTe Single Crystal: Explore of Strain-sensitivity Inspection Techniques. *Physics Procedia*. 76, 4-10. doi:10.1016/j.phpro.2015.10.002

Available online at www.sciencedirect.com

ScienceDirect

Physics Procedia 76 (2015) 4 – 10

Physics Procedia

The 17th International Conference on Luminescence and Optical Spectroscopy of Condensed Matter (ICL2014)

Detection sensitivities of photoluminescence spectroscopy and polariscopy to residual strains in a (110)-oriented ZnTe single crystal: Explore of strain-sensitivity inspection techniques

Hideo Takeuchi*

Department of Applied Physics, Graduate School of Engineering, Osaka City University, 3-3-138 Sugimoto, Sumiyoshi-ku, Osaka 558-8585, Japan

---

Abstract

We demonstrate that sensitivity of polariscopy to residual strains is higher than that of the photoluminescence spectroscopy in a (110)-oriented ZnTe single crystal. We carried out x-ray topography and micro θ-2θ x-ray diffraction measurements in order to thoroughly clarify the crystal quality connecting with the residual strains. The two x-ray analyses revealed that there is misalignment from the [110] direction in some regions of the present sample. We found the following main results: The polariscopic analysis detects the residual strain formed by the misalignment, whereas the photoluminescence measurement cannot detect the residual strain. Thus, we conclude that polariscopy has the sensitivity to the residual strain higher than that of the photoluminescence spectroscopy. We confirmed that the polariscopic analysis can detect the internal strain less than 0.02% in the ZnTe crystal. In addition, we discuss the applicability of polariscopic analysis to other compound semiconductors.

Peer-review under responsibility of The Organizing Committee of the 17th International Conference on Luminescence and Optical Spectroscopy of Condensed Matter

Keywords: ZnTe; residual strains; x-ray topography; micro θ-2θ x-ray diffraction; photoluminescence spectroscopy; polariscopy; inspection techniques

---

* Corresponding author. Tel.: +81-6-6605-2174; fax: +81-6-6605-2174.
E-mail address: takeuchi@a-phys.eng.osaka-cu.ac.jp

Peer-review under responsibility of The Organizing Committee of the 17th International Conference on Luminescence and Optical Spectroscopy of Condensed Matter
doi:10.1016/j.phpro.2015.10.002

1. Introduction

Ultrafast response of nonlinear optical crystals has considerable significance on cutting-edge photonics: terahertz optoelectronics (Sakai 2005). Recent progresses in femtosecond-pulse-laser systems have been enabling time-domain terahertz spectroscopy. The application of terahertz spectroscopy covers biological system imaging, innovative drug development, security system, and metamaterial investigation. Terahertz waves are useful spectroscopic probing tools to investigate novel physics of condensed matters (Lee 2008). In terahertz spectroscopy, essential optical components are terahertz-wave emitters and detectors, of the operation principles which connect with ultrafast phenomena. For the terahertz emitters, the utilizations of photoconductive antennas (Auston 1983) and semiconductor surfaces (Zhang and Auston 1992) are proposed. The nonlinear optical crystals also have a capability of generating the terahertz wave. The second electric susceptibility tensor of the nonlinear optical crystal produces optical rectification in illuminating the femtosecond laser pulses, triggering the generation of the terahertz wave. Various nonlinear optical crystals have been examined for achieving the intense terahertz waves (Auston et al. 1984; Hu et al. 1990; Han and Zhang 1998; Huber et al. 2000; Blanchard et al. 2007; Hirori et al. 2011). The nonlinear optical crystals are also are utilized as the detectors for the terahertz wave. This is because they are suitable for the electro-optic sampling (Wu and Zhang 1995; Wu and Zhang 1996). The mechanism of the electro-optic sampling is based on the Pockels effect (Lee 2008, p.92): the optical birefringence due to the externally applied electric fields. The Pockels effect has the same nonlinear optical coefficient as the optical rectification (Boyd 2008, Chapter 11). Accordingly, the nonlinear optical crystals, which were the targets of the investigation of References (Auston et al. 1984; Hu et al. 1990; Han and Zhang 1998; Huber et al. 2000; Blanchard et al. 2007; Hirori et al. 2011), are employed in the electro-optic sampling. Among various nonlinear optical crystals for terahertz spectroscopy, (110)-oriented ZnTe crystals, of the thicknesses which are several hundred micrometers, are widely used owing to its large electro-optic coefficient γ_{41}: 4.0×10^{-12} m/V (Boyd 2008, p.517). In addition, it is relatively easy to obtain the velocity matching condition at the typical operational wavelength (about 800 nm) of Ti:sapphire femtosecond pulse lasers (Lee 2008, pp. 87-90). Wu *et al.* demonstrated the two-dimensional electro-optic imaging of the terahertz beam with use of the ZnTe crystal (Wu et al. 1996). Usami *et al.* developed a real-time terahertz imaging system based on the two-dimensional electro-optic sampling (Usami et al. 2002). They obtained the terahertz images using a charge-coupled-detection camera at the video rate up to 30 frames per second, and observed moving objects. The referenced reports indicate the high advantage of the ZnTe crystals in the terahertz spectroscopic measurement. The two-dimensional electro-optic sampling requires the following characteristics to the ZnTe crystal: being free from residual strains. The residual strain leads to the emergence the photoelastic effect. The photoelastic effect also causes the optical birefringence, so that the terahertz image is disturbed from the ideal image. In addition, the residual strain forms the warp in the ZnTe crystal, resulting in the deviation from the flatness. Accordingly, it is essential and meaningful to evaluate the residual strain.

The strain evaluations are widely performed using the photoluminescence measurement in the research and development fields of semiconductors. In measuring photoluminescence spectra, the residual strain is reflected to the peak photon energy of the band due to the interband transition and/or exciton transition. The peak energy of the band originating from these transitions is shifted by the stress corresponding to the strain through the deformation potential (Pelant 2012). The photoluminescence map of the semiconductor wafer is used to evaluate the strain distribution. We, on the other hand, point out other choices for evaluating the residual strain: Polariscopy (Whalstom 1951; Cloud 1994; Kompaneĭtsev 2006). The polariscopic analysis is applicable to the samples transparent to the light. The residual strain causes the refractive index anisotropy, which forms the fast and slow axes. The formation changes the polarization direction of the light. In the polariscopic measurement, the sample is placed between the polarizer and analyzer aligned in the crossed-Nicol (or referred as cross-Nicol) configuration. The magnitude of the strain is recorded as the intensity of the transmitted light. Since the fundamental transition energy of ZnTe is 2.26 eV at room temperature (Larch 1957; Madelung 1982), the incoming light with the wavelength longer than 550 nm transmits through the ZnTe crystal. Accordingly, the polariscopic analysis has a potential for the evaluation of the ZnTe crystal.

In the present paper, we compare the strain sensitivity of polariscopy with that of photoluminescence spectroscopy. We systematically performed the present investigation. We, in advance, carried out reflection-type x-ray topography and micro θ-2θ x-ray diffraction measurement. This is because, for discussing the evaluation methods, it is essential to thoroughly reveal the sample characterisics. In the x-ray topograph of the present sample, we observed the undulation formed by missing of colour. From the result of the micro θ-2θ x-ray diffraction measurement, we confirmed that the region corresponding to the undulation pattern coincides with the appearance of the region misaligned from the [110] direction. We found that the inhomogeneous light transmission pattern in the polariscopic map appears in the undulated region of the x-ray topograph. In contrast, we observed it in the photoluminescence spectra that the peak photon energy of the photoluminescence band, which results from the interband transition, is not shifted. We estimate the strain-sensitivity limit of the photoluminescence measurement taking account of the deformation potential effect. Furthermore, we discuss the effectiveness of the polariscopic analysis, and demonstrate its suitability to the inspection technique of various semiconductors.

2. Sample and experimental procedures

The present sample was a commercially purchased (110)-oriented ZnTe single crystal chip with the size of 1.0 cm × 1.1 cm. The thickness was 500 μm. As shown in Fig. 1, the optical photograph of the present sample had complete uniformity: The light scattering did not exist. The reflection type x-raytopograph (Cullity 1978) of the sample was obtained with use of the Cu Kα x-ray line. The diffraction plane was a (531) plane and the slit width was 1.0 mm. The micro θ-2θ x-ray diffraction pattern was measured using the Co Kα line. The 2θ angle ranged from 15 to 80 degrees. The polariscopic measurement was performed in the crossed-Nicol configuration, using a linear polarizer and analyzer. The sample was inserted between the analyzer and polarizer. The light source was a white light-emitting-diode panel. The image, reflecting the intensity of the light transmitted through the analyser, was taken with use of a conventional digital still camera. In the photoluminescence measurement, the photon energy and power of the excitation laser beam were 2.81 eV and 0.1 mW, respectively, and the spot size was 50 μm in diameter at the sample surface. The spectral resolution power was 0.2 nm in wavlength. All the measurements were performed at room temperature.

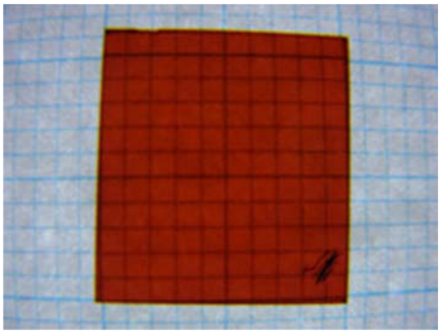

Fig. 1. Optical photograph of the present sample. The scattering of the light is not observed. The pattern appearing at the under right corner is due to the mark.

3. Experimental Results and Discussion

Figure 2 shows the x-ray topograph of the present sample. It is apparent that the undulation is detected. The undulation is considerably large in the upper right corner side. Since the inhomogeneous brightness of the x-ray topograph connects with the disturbance magnitude of the crystal-axis orientation, the appearance of the undulation suggests the presence of misalignment from the [110] direction. For elucidating the origin of the undulation pattern in the x-ray topograph, we performed the micro θ-2θ x-ray diffraction measurement. Figure 3 shows the micro θ-2θ x-ray diffraction patterns at the under left corner and upper right corner in the x-ray topograph. The x-ray diffraction pattern, which is observed at the under left corner, exhibits the reflection lines at the 2θ angles of 44 and 49 degrees. The lattice constant of ZnTe is 0.6102 nm (Madelung 1982), so that the observed lines are assigned to the (220) reflection of the Co Kβ1 line and the (220) reflection of the Co Kα line, in order of increasing 2θ angle. The observation of the (220)-reflection line is reasonable because the present sample is oriented to the [110] direction. In the x-ray diffraction pattern at the upper right corner, the additional line is detected at 28 degrees. The origin of this line is attributed to the (111) reflection of the Co Kα line. The appearance of the (111)-reflection line indicates the formation of the misalignment from the [110] direction. The intensity of the (111)-reflection line is weaker by the factor of 10^2 than that of the (220)-reflection line; namely, the misalignment is quite small. This extinguishes the light scattering in the optical photograph of the present sample as shown in Fig. 1. The same results for other materials were reported obtained in the earlier works (Takeuchi 2011; Takeuchi 2013).

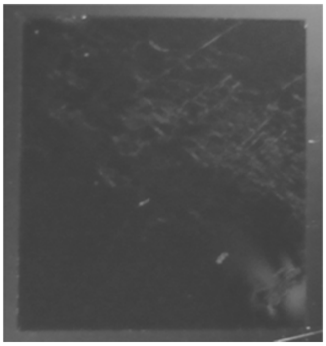

Fig. 2. Reflection type x-ray topograph of the sample. The undulation appears at the upper right corner.

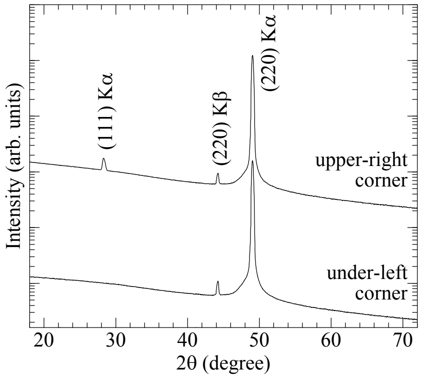

Fig. 3. Micro 2θ-2θ x-ray diffraction patterns at the under left corner and upper right corner in the x-ray topograph. Only the (220)-reflection lines are observed at the under left corner in the x-ray topograph, the additional (111) reflection line is detected at the upper right corner.

Next, we compare the residual strain sensitivity of the polariscopic analysis with that of the photoluminescence measurement. The polariscopic image is shown in Fig. 4. The inhomogeneous light transmission is clearly observed at the upper right corner region that exhibits the undulation pattern in the x-ray topograph. The crossed-Nicol configuration has a selection rule that the linearly polarized light is forbidden to transmit from the analyzer in the ideal zincblende crystals. The observed light transmission, therefore, indicates the presence of the refractive index anisotropy mainly originating from the residual strain. We also note that the light transmission is secondarily caused by the light scattering at the boundary of misoriented planes; however, this effect is minor because of the uniform optical photograph is observed as shown in Fig. 1.

Following the polariscopic analysis, we carried out the photoluminescence measurement. Figure 5 shows the photoluminescence spectra at the under left corner and upper right corner. Each photoluminescence band shows the peak at the photon energy of 2.26 eV that corresponds to the interband transition energy at room temperature. The observed bands are, therefore, attributed to the photoluminescence from the interband transition. As shown in Fig. 5, each peak photon energy of the photoluminescence band is the same within the spectral resolution power, indicating the quite low sensitivity of the photoluminescence measurement to the residual strain. Thus, we conclude that the polariscopic analysis has the internal strain sensitivity higher than the photoluminescence measurement.

Finally, we discuss the highest limit of the strain sensitivity. The peak energy shift of the photoluminescence band ΔE is proportional to the relative variation of the unit-cell volume $\Delta V/V$:

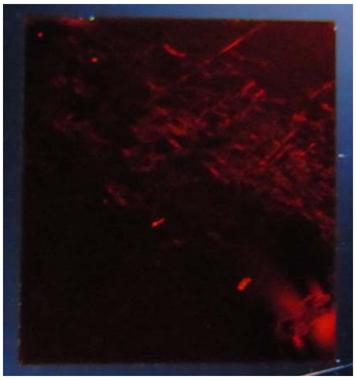

Fig. 4. The polariscopic image. The inhomogeneous light transmission is clearly observed at the upper right corner region that exhibits the undulation pattern in the x-ray topograph.

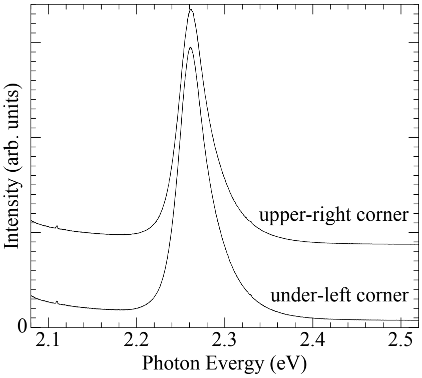

Fig. 5. Photoluminescence spectra at the under left corner and upper right corner at room temperature. The band peaking at 2.26 eV originates from the interband transition at the Γ point of the Brillouin zone.

$$\Delta E = \alpha \frac{\Delta V}{V} \tag{1}$$

In Eq. (1) the quantity α is the hydrostatic deformation potential, where the value of a is -5.53 eV (Bertho et al. 1991). The spectrum resolution of the present photoluminescence measurement was 0.2 nm that corresponds to 1 meV in the present wavelength range. Taking account of this value, the relative variation of the unit-cell volume is less than 0.02% in the present sample. Accordingly, it is reasonable to deduce that the polariscopic measurement has the ability to sensitively detect the strain less than 0.02%. Thus, we conclude that the polariscopic measurement is a highly sensitive method for detecting the strains in the ZnTe single crystals.

We also estimate the pressure p that corresponds to the relative variation of the volume $\Delta V/V$. The pressure p is expressed by the following relation,

$$\Delta p = B\frac{\Delta V}{V} \tag{2}$$

where the quantity B is the bulk modulus. The value of B for ZnTe is 5.08×10^{11} dyn/cm^2 (Lee 1970). The relative variation of the volume is 0.02% corresponds to the pressure of 1.1×10^{8} dyn/cm^2 (11 MPa). In usual, the band-gap energy shift is observable in the pressure is of the order of gigapascal. We note that the present polariscopic measurement was performed at room temperature with simple polarizing plate. Taking account of the above-mentioned facts, we reach a conclusion that the polariscopic analysis has a highly sensitive and convenient characterization for the relatively low residual strains.

Table 1. Hydrostatic deformation potentials of the typical zincblende compound semiconductors (Van de Walle 1989).

	Hydrostatic deformation potential (eV)
InAs	-6.08
GaP	-8.83
InP	-6.31
GaSb	-7.64
ZnSe	-5.83
ZnS	-5.83
CdTe	-4.52
HgTe	-4.48

Table 2. Hydrostatic deformation potentials of the typical wurtzite compound semiconductors.

	Hydrostatic deformation potential (eV)
GaN [a)]	-8.16
AlN [b)]	-7.1
ZnO [c)]	−4.47

From (a) Gil 1995; (b) Blanchard 1997; (c) Karzel 1996.

It is meaningful to discuss that the polariscopic analysis is applicable to other semiconductors. Table 1 and Table 2 list the hydrostatic deformation potentials of the typical compound semiconductors. The value of the hydrostatic potential is the same order as that of ZnTe. The resent progress in wide band-gap semiconductor devices stimulates the high yield of the single-crystal wafers for substrates. The residual strain is still a crucial problem. The polariscopic analysis provides a solution of inspecting the residual strain distribution in the wafers of various compound semiconductors if the residual strain is not evaluated using the photoluminescence measurement owing to the detection limit.

4. Summary

We have systematically investigated the residual strain sensitivities of polariscopy and photoluminescence spectroscopy in the (110)-oriented ZnTe crystal. We have used the reflection-type x-ray topographic measurement and micro θ-2θ x-ray diffraction measurement, enabling the detailed residual strain investigation. We have observed the undulation in the x-ray topograph, the position of which contains the misalignment from the [110] direction according to the results of the x-ray diffraction measurement. The polariscopic analysis has been clarified that, in the undulated region of the x-ray topograph, the light incident to the sample inhomogeneously transmits from the analyzer. The light transmission indicates that the refractive index anisotropy is produced by the residual strain. The photoluminescence measurement, however, has been revealed to be insensitive to the internal strain. Thus, we reach a conclusion that the polariscopic analysis has the residual strain sensitivity higher than the photoluminescence measurement. From the strain-detection limit of the photoluminescence measurement, we have deduced that the polariscopic analysis detects the strain less than 0.02%.

References

Auston, D. H., 1983. Subpicosecond Electro-Optic Shock Waves. Applied Physic Letters 43, 713.

Auston, D. H., Cheung, K. P., Valdmanis, J. A., and Kleinman, D. A., 1984. Cherenkov Radiation from Femtosecond Optical Pulses in Electro-Optic Media. Physical Review Letters 53, 1555.

Bertho, D., Boiron, D., Simon, Jouanin, A. C., and Priesta, C., 1991. Calculation of Hydrostatic and Uniaxial Deformation Potentials with a Self-Consistent Tight-Binding Model for Zn-cation-based II-VI Compounds. Physical Review B 44, 6118.

Blanchard, F., Razzari, L., Bandulet, H. -C., Sharma, Morandotti, G., R., Kieffer, J. -C., Ozaki, Reid, T. M., Tiedje, H. F., Haugen, H. K., and Hegmann. F. A., 2007. Generation of 1.5 μJ Single-cycle Terahertz Pulses by Optical Rectification from a Large Aperture ZnTe Crystal. Optics Express 15, 13212-13220.

Boyd, R. W., "*Nonlinear Optics 3rd edition*", 2008. Academic Press, Massachusetts, Chapter 11.

Brunner, D., Angerer, H., Bustarret, E., Freudenberg, F., Höpler, R., Dimitrov. R., Ambacher, O. and Stutzmann, M., 1997. Optical constants of epitaxial AlGaN films and their temperature dependence. Journal of Applied Physics 82, 5090.

Cloud, G., "*Optical Methods of Engineering Analysis"*1994. Cambridge University Press, Chapter 4.

Cullity, B. D.,"*Elements of X-Ray Diffraction -2nd Edition*" 1978. Addison-Wesley, Massachusetts.

Gil, B., Briot, O., Aulombard and R.-L., 1995. Valence-band Physics and the Optical Properties of GaN Epilayers Grown onto Sapphire with Wurtzite Symmetry. Physical Review B 52, R17028.

Han, P. Y., and Zhang, X.-C., 1998. Coherent, Broadband midinfrared Terahertz Beam Sensors. Applied Physics Letters 73, 3049.

Hirori, H., Doi, A., Blanchard, F., and Tanaka, K., 2011. Single-cycle Terahertz Pulses with Amplitudes Exceeding 1 MV/cm Generated by Optical Rectification in $LiNbO_3$. Applied Physics Letters 98, 091106.

Hu, B. B., Zhang, X.-C., Auston, D. H., and Smith, P. R., 1990. Free-space Radiation from Electro-optic Crystals. Applied Physics Letters 56, 506.

Huber, R., Brodschelm, A., Tauser, F., and Leitenstorfer, A., 2000. Generation and Field-resolved Detection of Femtosecond Electromagnetic Pulses Tunable up to 41 THz. Applied Physics Letters 76, 3191.

Karzel, H., Potzel, W., Köfferlein, Schiessl, M., W., Steiner, M., Hiller, U., Kalvius, G. M., Mitchell, D. W., Das, T. P., Blaha, P., Schwarz, K., and Pasternak, M. P,. 1996., Lattice Dynamics and Hyperfine Interactions in ZnO and ZnSe at High External Pressures. Physical Review B 53 11425.

Kompaneĭtsev, V. P., 2006. Isogyre Equation for Uniaxial and Biaxial Crystals. Crystallography Reports 51, 640.

Larach, S., Schrader, R. E., and Stocker, W., 1957. Anomalous Variation of Band Gap with Composition in Zinc Sulfo- and Seleno-Tellurides. Physical Review B 108, 587.

Lee, B.H., 1970. Pressure Dependence of the Second-order Elastic Constants of ZnTe and ZnSe. Journal of Applied Physics 41, 2988.

For a review, Lee, Y.-S., "*Principles of Terahertz Science and Technology"*, Springer-Verlag, Berlin, 2008, and references therein.

Madelung, O., Rössler, U., Schulz, M., (Eds.) "*Landolt-Börnstein -Group III Condensed Matter Numerical Data and Functional Relationships in Science and Technology*, 1982. Springer-Verlag, Berlin.

Pelant, I., and Valenta, J., "*Luminescence Spectroscopy of Semiconductors*", 2012. Oxford University Press, Oxford.

For a review, Sakai, K., (Ed.) 2005. "*Terahertz Optelectronics"*, Springer-Verlag, Berlin, and references therein.

Takeuchi, H., 2011. Circular Polariscopic Analysis of Strains in a Semi-insulating SiC Wafer: Its high Potential to Complement the Information Obtained from Monochromatic X-ray Topography. Review of Scientific Instruments 82, 033907.

Takeuchi, H., 2013. Enhancement Effects on Excitonic Photoluminescence Intensity Originating from Misaligned Crystal Blocks and Polycrystalline Grains in a ZnO Wafer. The European Physical Journal B 86:50.

Usami, M., Iwamoto, T., Fukasawa, R., Tani, M., Watanabe, M., and Sakai, K., 2002. Development of a THz Spectroscopic Imaging System. Physics in Medicine and Biology 47, 3749.

Wahlstrom, E. E., *"Optical Crystallography"*, 1951. John Wiley & Sons, New York.

Van de Walle, C. G., 1989. Band lineups and deformation potentials in the model-solid theory. Physical Review B 39, 1871.

Wu, Q., Hewitt, T. D., and Zhang X. C-., 1996. Two-dimensional electro-optic imaging of THz beams. Applied Physics Letters 69, 1026.

Wu, Q., and Zhang, X. -C., 1995. Free-space Electro-optic Sampling of Terahertz Beams. Applied Physics Letters 67, 3525.

Wu, Q., and Zhang, X. -C., 1996. 7 Terahertz Broadband GaP Electro-optic Sensor. Applied Physics Letters, 70, 1784.

Zhang, X. -C., and Auston, D. H., 1992. Optoelectronic Measurement of Semiconductor Surfaces and Interfaces with Femtosecond Optics. Journal of Applied Physics 71, 326.